

Inhibition of CYP3A7 DHEA-S Oxidation by Lopinavir and Ritonavir: An Alternative Mechanism for Adrenal Impairment in HIV Antiretroviral-Treated Neonates

Sylvie E. Kandel and Jed N. Lampe*

Cite This: *Chem. Res. Toxicol.* 2021, 34, 1150–1160

Read Online

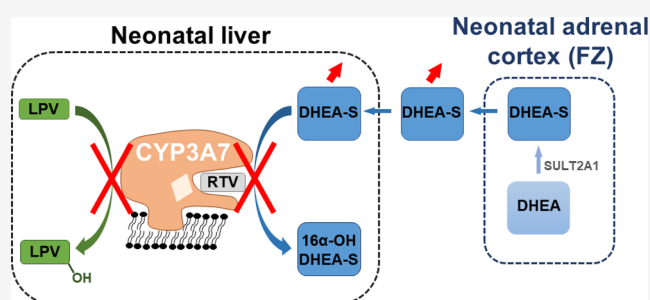
ACCESS |

Metrics & More

Article Recommendations

Supporting Information

ABSTRACT: Prophylactic antiretroviral therapy (ART) in HIV infected pregnant mothers and their newborns can dramatically reduce mother-to-child viral transmission and seroconversion in the neonate. The ritonavir-boosted lopinavir regimen, known as Kaletra, has been associated with premature birth and transient adrenal insufficiency in newborns, accompanied by increases in plasma dehydroepiandrosterone 3-sulfate (DHEA-S). In the fetus and neonates, cytochrome P450 CYP3A7 is responsible for the metabolism of DHEA-S into 16 α -hydroxy DHEA-S, which plays a critical role in growth and development. In order to determine if CYP3A7 inhibition could lead to the adverse outcomes associated with Kaletra therapy, we conducted *in vitro* metabolic studies to determine the extent and mechanism of CYP3A7 inhibition by both ritonavir and lopinavir and the relative intrinsic clearance of lopinavir with and without ritonavir in both neonatal and adult human liver microsomes (HLMs). We identified ritonavir as a potent inhibitor of CYP3A7 oxidation of DHEA-S ($IC_{50} = 0.0514 \mu M$), while lopinavir is a much weaker inhibitor ($IC_{50} = 5.88 \mu M$). Furthermore, ritonavir is a time-dependent inhibitor of CYP3A7 with a K_i of $0.392 \mu M$ and a k_{inact} of 0.119 min^{-1} , illustrating the potential for CYP3A mediated drug–drug interactions with Kaletra. The clearance rate of lopinavir in neonatal HLMs was much slower and comparable to the rate observed in adult HLMs in the presence of ritonavir, suggesting that the addition of ritonavir in the cocktail therapy may not be necessary to maintain effective concentrations of lopinavir in neonates. Our results suggest that several of the observed adverse outcomes of Kaletra therapy may be due to the direct inhibition of CYP3A7 by ritonavir and that the necessity for the inclusion of this drug in the therapy may be obviated by the lower rate of lopinavir clearance in the neonatal liver. These results may lead to a reconsideration of the use of ritonavir in neonatal antiretroviral therapy.



INTRODUCTION

Prevention of mother-to-child human immunodeficiency virus (HIV) transmission during pregnancy, delivery, and breastfeeding by using antiretroviral therapy (ART) has proven to be extremely beneficial in reducing the number of new HIV-1 infections in children.^{1–3} The antiretroviral (ARV) drug regimens used for pregnant women and neonates include nucleoside reverse transcriptase inhibitors (NRTIs), non-nucleoside reverse transcriptase inhibitors (NNRTIs), protease inhibitors (PIs), or integrase strand transcriptase inhibitors (INSTIs) with treatment frequency and duration dependent on the risk factors involved.^{4,5} However, these treatments have their challenges with modulating metabolic pathways in both the mother and the newborn resulting in dyslipidemia, glucose intolerance, and abnormal mitochondrial function or adrenal dysfunction.^{6–9} The PI ritonavir-boosted lopinavir regimen, also known as Kaletra, is used during pregnancy or as a prophylactic treatment for neonates and has been associated with premature birth and transient adrenal insufficiency in newborns.^{7,10–12} Previous studies have shown elevated plasma

concentrations of adrenal steroid hormones including 17 α -hydroxy progesterone (17-OHP), dehydroepiandrosterone (DHEA), and dehydroepiandrosterone 3-sulfate (DHEA-S) in neonates receiving the Kaletra treatment (Figure 1).^{7,8,13} Several hypotheses regarding the mechanism of adrenal hormonal imbalance and the associated life-threatening symptoms observed in newborns subjected to Kaletra therapy have been proposed. One of the excipients of Kaletra is propylene glycol, and while it is not known to effect steroidogenesis,¹⁴ it has been proposed that the alcohol properties of the compound may be responsible for some of the harmful effects including heart, kidney, and breathing complications.¹² A mechanism for the alteration of the adrenal

Received: January 15, 2021

Published: April 6, 2021



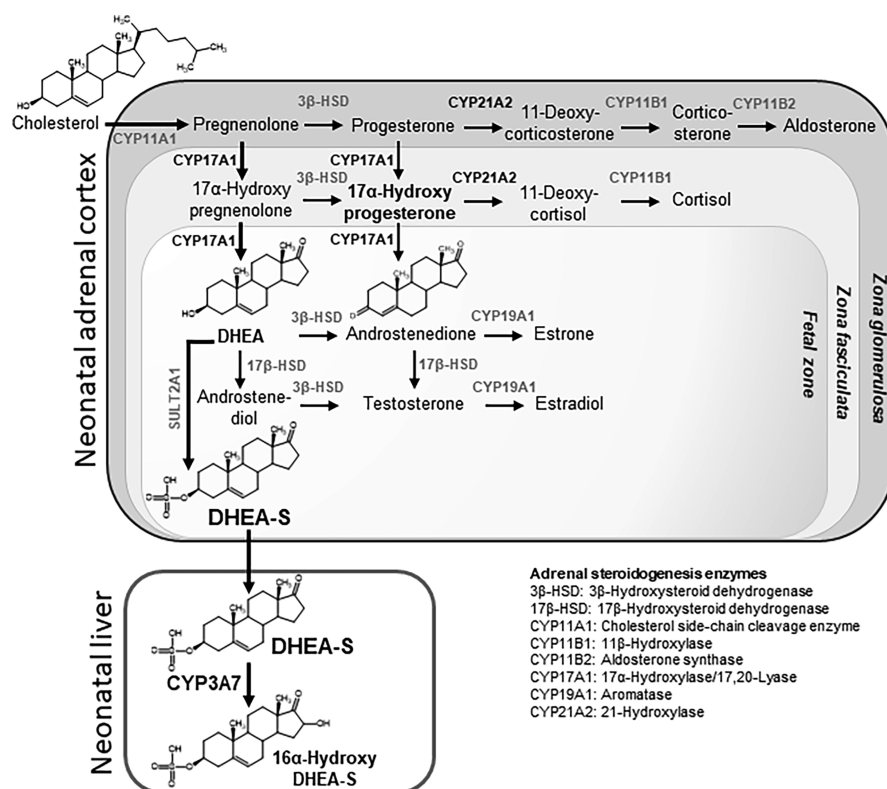


Figure 1. Neonatal adrenal steroid synthesis and hepatic metabolism of DHEA-S.

hormonal profile was proposed by Kariyawasam et al. in 2020 who demonstrated moderate inhibition by lopinavir, but not ritonavir, of two adrenal cytochrome P450 (CYP) enzymes, CYP17A1 and CYP21A2, in NCI-H295R cells.¹³ This could point to a mechanism that may explain many of the clinical pathologies associated with Kaletra treatment. However, ritonavir and lopinavir are much more effective inhibitors of CYP3A4, the CYP enzyme predominantly associated with their clearance *in vivo*, than other CYP enzymes.^{11,15–17} Interestingly, CYP3A4 is virtually absent in the neonate, while CYP3A7 is the dominant CYP3A subfamily enzyme present and is responsible for the clearance of drugs through the CYP3A enzymatic pathway.^{18–23} Nevertheless, the primary role of CYP3A7 is the oxidation of DHEA-S to 16 α -hydroxydehydroepiandrosterone 3-sulfate (16 α -hydroxy DHEA-S),^{24,25} an important intermediate in the estriol biosynthetic pathway. In the pregnant mother, 16 α -hydroxy DHEA-S is exported to the placenta where it subsequently undergoes desulfation and a series of oxidations to ultimately form estriol, which is critically important in bringing the pregnancy to full term.^{26,27} Women with low estriol levels are far more likely to give birth to premature and even stillborn infants.²⁸ Furthermore, the level of 16 α -hydroxy DHEA-S is an important indicator for normal growth and development of the neonate.²⁹ Inhibition of CYP3A7, therefore, could cause irrevocable harm to the developing fetus. While the involvement of the hepatic CYP3A enzymes in the deleterious side effects of Kaletra has been postulated in previous studies,^{7,8} to our knowledge no research has been conducted to examine the impact of CYP3A7 inhibition by lopinavir and ritonavir on endogenous DHEA-S metabolism. Given that ritonavir is a potent inhibitor of CYP3A4, it is a reasonable hypothesis that it is highly likely to also inhibit CYP3A7 and

interfere with the oxidation of DHEA-S. Therefore, we set out to test if this was indeed the case and, if so, to determine the mode and quantitative extent of the inhibition. Similarly, since both ritonavir and lopinavir are dosed together, we also sought to determine the CYP3A7 inhibition parameters associated with lopinavir as well. In the adult, lopinavir is primarily cleared by CYP3A4. Ritonavir is included as an adjuvant for its properties as a potent CYP3A4 inhibitor, thereby improving the pharmacokinetic profile of lopinavir.^{11,30} However, there is no data currently available in the literature regarding lopinavir clearance in the neonatal liver. Given that CYP3A7 is the main CYP3A isoform present in the neonatal liver, and that it has critical physiological functions, it is important to understand if differences in lopinavir clearance exist between the CYP3A4 and CYP3A7 enzymes. Therefore, in this study we also characterized the intrinsic clearance of lopinavir for the recombinant CYP3A4 and CYP3A7 enzymes and for adult and neonatal pooled human liver microsomes.

EXPERIMENTAL PROCEDURES

Materials. The DHEA-S standard was purchased from Cayman Chemical (Ann Harbor, MI). The metabolite standard, 16 α -hydroxy DHEA-S, was purchased from Steraloids (Newport, RI). Glucose-6-phosphate, glucose-6-phosphate dehydrogenase, β -nicotinamide adenine dinucleotide phosphate (NADP⁺), and the internal standard, dehydroepiandrosterone-*d*₅-3-sulfate (DHEA-S-*d*₅), were obtained from Sigma-Aldrich (St. Louis, MO). Lopinavir, ritonavir, and saquinavir mesylate were purchased from Toronto Research Chemicals (North York, ON, Canada). All other chemicals and solvents used were obtained from standard suppliers and were of reagent or analytical grade. The CYP3A4 (catalog number: 456202) and CYP3A7 Supersomes (catalog number: 456237) were purchased from Corning (Corning, NY) where the recombinant CYP3A enzymes were coexpressed with the human cytochrome P450

reductase and the human cytochrome b5 in Sf9 insect cells using a baculovirus expression system.

Adult and Neonatal Human Liver Microsomes. Adult human liver microsomes (HLMs) were purchased from Sekisui XenoTech, LLC (Kansas City, KS). XTreme 200 mixed gender adult HLMs (catalogue number: H2610) were used for this study.

The neonatal liver tissues were donations from the Liver Center of the University of Kansas, Medical Center and were between 5 and 10 days of age. Neonatal HLMs were prepared following the method described by Pearce et al. (1996) with slight modifications.³¹ In brief, frozen neonatal liver tissue samples were weighed and transferred in homogenization buffer (50 mM Tris-HCl buffer, pH 7.4, 150 mM potassium chloride, and 2 mM ethylenediaminetetraacetic acid [EDTA]) to thaw. The liver tissues were minced thoroughly on ice and further processed using a tissue Tearor (3 × 5 s). A Teflon-glass homogenizer was used to further homogenize the liver tissues (6–8 strokes). The liver homogenate samples were then centrifuged for 20 min at 12,000 × *g* and 4 °C in an Eppendorf 5910R centrifuge to remove unbroken cells, nuclei, mitochondria, and lysosomes. The supernatants, corresponding to the cytosolic and microsomal fractions, were then centrifuged for 1 h at 105,000 × *g* and 4 °C in a Beckman L-80 ultracentrifuge with a Sorvall 50.2 Ti rotor (Sorvall, Newton, CT). The upper lipid bilayer was removed with a cotton swab, and the cytosolic supernatants were collected. The microsomal pellets were resuspended in wash buffer (150 mM potassium chloride and 10 mM EDTA) and homogenized with a Teflon-glass homogenizer. The microsomal suspension samples were further centrifuged for 1 h at 105,000 × *g* and 4 °C in a Beckman ultracentrifuge with a Sorvall 50.2 Ti rotor. The resulting microsomal pellets were homogenized in 250 mM sucrose and stored at –80 °C. The neonatal HLM protein concentrations were determined using a Pierce bicinchoninic acid (BCA) protein assay kit (Thermo Fisher Scientific, Waltham MA). A pool of three neonatal HLMs was prepared by combining microsomes based on an equal protein amount for each. The neonatal HLMs were assessed for CYP3A and CYP4A11 enzyme activities using midazolam and lauric acid as probe substrates, respectively, and metabolite formation was determined by liquid chromatography tandem mass spectrometry (LC-MS/MS) analysis (data not shown).

Recombinant CYP3A7 *In Vitro* Activity and Inhibition Assays for DHEA-S. The kinetic reactions (250 μL) evaluating DHEA-S metabolism by the recombinant CYP3A7 Supersomes contained various concentrations of DHEA-S (2.5–120 μM) dissolved in methanol (0.5% v/v), CYP3A7 Supersomes (10 pmol/mL), 100 mM potassium phosphate buffer (pH 7.4), and 3 mM MgCl₂. After an equilibration at 37 °C for 3 min, the reactions, prepared in triplicate, were initiated by the addition of a NADPH-regenerating system mix consisting of NADP⁺ (1 mM), glucose-6-phosphate (10 mM), and glucose-6-phosphate dehydrogenase (2 IU/mL). The reactions were incubated for 10 min at 37 °C under agitation and were stopped by the addition of ice-cold methanol (250 μL) containing 100 ng/mL DHEA-S-*d*₃ internal standard. The reactions were done under steady state kinetics based on a prior time and protein experiment establishing linearity up to a 20 min incubation time (data not shown). Incubations without the NADPH-regenerating system mix served as negative controls. Precipitated proteins were collected by centrifugation of the stopped reaction samples for 10 min at 1,800 × *g* and 4 °C. Supernatants were transferred to high performance liquid chromatography (HPLC) vials, and aliquots of 5 μL were analyzed by LC-MS/MS. The 16α-hydroxy DHEA-S metabolite was quantified based on a calibration curve ranging from 0.025 to 10 μM.

Similar assay conditions were used for the inhibition reactions with the HIV protease inhibitors and the recombinant CYP3A7 Supersomes except that the concentration of DHEA-S was set to 5 μM, and the reaction volume was 200 μL. The concentration ranges tested for lopinavir and ritonavir, dissolved in methanol, were 0.05 to 100 μM and 0.0005 to 1 μM, respectively. Solvent control (methanol) was used as the 100% control activity. Methanol concentration in the final incubation reactions was 1% (v/v).

For ritonavir time-dependent inhibition, recombinant CYP3A7 Supersomes (100 pmol/mL) were preincubated in triplicate with ritonavir at 0.01, 0.05, 0.1, 0.25, 0.5, and 1 μM in 100 mM potassium phosphate buffer (pH 7.4) and 3 mM MgCl₂. Ritonavir was dissolved in methanol (0.4% v/v), and solvent control (methanol) was used as the 100% control activity. The preincubation reactions (final volume of 240 μL) were started by the addition of the NADPH-regenerating system mix. After 0, 8, 16, 24, and 32 min at 37 °C, a 20 μL aliquot of the recombinant CYP3A7/ritonavir preincubation was transferred to a 50 μM DHEA-S reaction (180 μL) containing 100 mM potassium phosphate buffer (pH 7.4), 3 mM MgCl₂, and the NADPH-regenerating system mix. The DHEA-S incubations were stopped after 8 min at 37 °C by the addition of ice-cold methanol (200 μL) containing 100 ng/mL DHEA-S-*d*₃ internal standard. Precipitated proteins were collected by centrifugation of the stopped reaction samples for 10 min at 1,800 × *g* and 4 °C. Supernatants were transferred to HPLC vials, and aliquots of 5 μL were analyzed by LC-MS/MS for formation of the 16α-hydroxy DHEA-S metabolite.

Inhibition of DHEA-S Metabolism in Neonatal Human Liver Microsomes by Lopinavir and Ritonavir. DHEA-S (50 μM) was incubated with neonatal pooled HLMs (0.05 mg/mL) in 1.8 mL reactions containing 100 mM potassium phosphate buffer (pH 7.4) and 3 mM MgCl₂. The inhibition effect of lopinavir (8 μM) without and with ritonavir (0.5 μM) was assessed for the formation of the 16α-hydroxy DHEA-S metabolite. The lopinavir concentration tested was near the C_{max} reported by Foissac et al. (2017), and ritonavir was about a 16-fold lower concentration than lopinavir as reported in the Kaletra package insert.^{32,33} After an equilibration at 37 °C for 3 min, the reactions, prepared in triplicate, were initiated by the addition of the NADPH-regenerating system mix. Incubation aliquots of 150 μL were transferred at 0, 5, 10, 15, 20, 25, and 30 min into ice-cold methanol (150 μL) (containing 50 ng/mL DHEA-S-*d*₃ as internal standard) to stop the enzymatic reaction. Solvent control incubations were prepared with a final methanol concentration at 0.5% (v/v). Additional incubations without the NADPH-regenerating system mix were done in parallel as negative controls. The samples were centrifuged for 20 min at 3,400 × *g* and 4 °C to remove precipitated proteins. Supernatants were transferred to HPLC vials, and aliquots of 2 μL were analyzed by LC-MS/MS. The 16α-hydroxy DHEA-S metabolite was quantified based on a calibration curve ranging from 0.01 to 10 μM.

Analytical Method for DHEA-S Hydroxylation. The DHEA-S incubation samples with the recombinant CYP3A7 enzyme and the neonatal HLMs were analyzed by LC-MS/MS with a Waters Acquity Ultra-Performance Liquid Chromatography (UPLC) system interfaced by electrospray ionization with a Waters Quattro Premier XE triple quadrupole (or a Xevo TQ-S micro tandem quadrupole) mass spectrometer (Waters Corp., Milford, MA) in negative ionization mode and with the multiple reaction monitoring (MRM) scan type. The following source conditions were applied: 3.5 (or 0.5) kV for the capillary voltage, 120 °C for the source temperature, 400 °C (or 450 °C) for the desolvation temperature, 50 L/h for the cone gas flow, and 600 (or 900) L/h for the desolvation gas flow. The following mass transitions, collision energies (CEs), and cone voltages (CVs) were used to detect the respective analytes: 383 > 97, CE = 30 V, CV = 50 V (or CE = 26 V, CV = 75 V) for the 16α-hydroxy DHEA-S metabolite, 367 > 97, CE = 30 V, CV = 45 V (or CE = 34 V, CV = 80 V) for DHEA-S, and 372 > 98, CE = 30 V, CV = 50 V (or CV = 75 V) for the internal standard DHEA-S-*d*₃. DHEA-S and its hydroxylated metabolite were separated on a Waters BEH C18 column (1.7 μm, 2.1 × 100 mm) by flowing 5 mM ammonium acetate in water and methanol at 0.4 mL/min. The following gradient was used: 30% organic (methanol) held for 0.5 min, increased to 98% over 3.5 min, and held at 98% for 0.9 min. The MS peaks were integrated using the QuanLynx software (version 4.1, Waters Corp., Milford, MA), and the analyte/internal standard peak area ratios were used for relative quantification. For determination of the hydroxy metabolite concentration, the regression fit was based on the analyte/internal standard peak area ratios calculated from the calibration

standards, and the analyte concentration in the incubations was back-calculated using a weighted ($1/x$) linear least-squares regression.

Enzyme Activity and Inhibition Kinetic Analysis. For the recombinant CYP3A7 DHEA-S kinetics experiment, mean metabolite formation rate values obtained from triplicate determinations were fit to the Michaelis–Menten (hyperbolic) and Hill (sigmoidal) equations using GraphPad Prism software (version 9.0.0, GraphPad Software, La Jolla, CA). For the lopinavir and ritonavir IC₅₀ experiments with the recombinant CYP3A7 enzyme, the mean analyte/internal peak area ratio for the 16 α -hydroxy DHEA-S metabolite was determined for the solvent control samples and was referred to as 100% control activity to calculate the percent remaining activity in samples containing increasing concentrations of HIV protease inhibitors. GraphPad Prism software was used for dose–response curve fitting. The mechanism-based inactivation data were analyzed using the standard replot method, although other modeling methods have emerged for determination of the inactivation kinetic parameters.^{34–37} The percentage of CYP3A7 remaining activity was determined based on the analyte/internal peak area ratios using the solvent control at a corresponding preincubation time as the 100% activity. The observed inactivation rate constant (k_{obs}) was estimated using linear fit of the mean natural logarithm of the remaining activity versus the preincubation time. The mechanism-based inactivation constants k_{inact} and K_I were determined based on the k_{obs} versus the ritonavir concentration in the preincubation using GraphPad Prism for curve fitting.

Lopinavir Intrinsic Clearance by Recombinant CYP3A Enzymes. Lopinavir (1 μM) was incubated in triplicate with recombinant CYP3A7 or CYP3A4 Supersomes (2 or 40 pmol/mL) in a 2.2 mL reaction containing 100 mM potassium phosphate buffer (pH 7.4) and 3 mM MgCl_2 . Methanol concentration in the final incubation reactions was 1% (v/v). The difference in the protein content was corrected by the addition of Supersomes insect cell control microsomes (catalog number: 456200) to obtain a constant protein concentration of 0.48 mg/mL. After a 3 min equilibration at 37 $^\circ\text{C}$, the reactions were started by the addition of the NADPH-regenerating system mix. Incubation aliquots of 150 μL were transferred at 0, 10, 20, 30, 40, and 50 min into ice-cold methanol (150 μL) (containing 25 ng/mL saquinavir as internal standard) to stop the enzymatic reaction. Incubations without the NADPH-regenerating system mix served as negative controls. Additional incubations containing ritonavir at 62.5 nM were done to evaluate the effect on lopinavir clearance. Precipitated proteins were collected by centrifugation of the stopped reaction samples for 10 min at $1,800 \times g$ and 4 $^\circ\text{C}$. Supernatants were transferred to HPLC vials, and aliquots of 5 μL were analyzed by LC-MS/MS.

Lopinavir Intrinsic Clearance by Neonatal and Adult Human Liver Microsomes. Lopinavir (1 μM) was incubated in triplicate with neonatal or adult pooled human liver microsomes at 0.02 and 0.1 mg/mL in 1.8 mL reactions containing 100 mM potassium phosphate buffer (pH 7.4) and 3 mM MgCl_2 . Methanol concentration in the final incubation reaction was 1% (v/v). After a 3 min equilibration at 37 $^\circ\text{C}$, the reactions were started by the addition of the NADPH-regenerating system mix. Incubation aliquots of 150 μL were transferred at 0, 5, 10, 15, 20, and 30 min into ice-cold methanol (150 μL) (containing 25 ng/mL saquinavir as internal standard) to stop the enzymatic reaction. Additional incubations without the NADPH-regenerating system mix were done in parallel as negative controls. Adult HLM incubations containing ritonavir at 62.5 nM were carried out to assess the effect on lopinavir clearance. The samples were centrifuged for 20 min at $3,400 \times g$ and 4 $^\circ\text{C}$ to remove precipitated proteins. Supernatants were transferred to HPLC vials, and aliquots of 1 μL were analyzed by LC-MS/MS.

Analytical Method for Lopinavir Clearance. The Waters Acquity UPLC system interfaced by electrospray ionization with a Waters Quattro Premier XE triple quadrupole (or a Xevo TQ-S micro tandem quadrupole) mass spectrometer (Waters Corp., Milford, MA) was used in the positive ionization mode and with the MRM scan type. The following source conditions were applied: 1.5 (or 1) kV for the capillary voltage, 120 $^\circ\text{C}$ for the source temperature, 450 $^\circ\text{C}$ for

the desolvation temperature, 50 L/h for the cone gas flow, and 600 (or 900) L/h for the desolvation gas flow. The following mass transitions, CEs, and CVs were used to detect the respective analytes: 629.5 > 183 (CE = 22 V; CV = 30 V) for lopinavir, 721.5 > 296 (CE = 20 V; CV = 35 V) for ritonavir, and 672 > 570 (CE = 32 V; CV = 40 V) for saquinavir, used as the internal standard. Protease inhibitors were separated on a Waters BEH C18 column (1.7 μm , 2.1×100 mm) by flowing 0.1% formic acid in water and acetonitrile at 0.5 mL/min. The following gradient was used: 30% organic (acetonitrile) held for 0.5 min, increased to 98% over 3.5 min, and held at 98% for 1.4 min. The MS peaks were integrated using QuanLynx software (version 4.1, Waters Corp., Milford, MA), and the analyte/internal standard peak area ratios were used for further calculations.

Intrinsic Clearance Analysis. In brief, the elimination rate constant (k) was estimated using a linear fit (GraphPad Prism software, v. 9.0.0) of the natural logarithm of the percent of lopinavir remaining versus time. Equations 1, 2, and 3 were used to calculate the *in vitro* half-life ($t_{1/2}$), intrinsic clearance for recombinant CYP ($\text{CL}_{\text{int,CYP}}$), and intrinsic clearance for HLMs ($\text{CL}_{\text{int,HLM}}$), respectively, with V representing the incubation volume, M_{P450} representing the moles of CYP enzyme in the recombinant incubations, and P_{HLM} representing the amount of protein in the HLM incubations.

$$t_{1/2} = \frac{\ln 2}{(-k)} \quad (1)$$

$$\text{CL}_{\text{int,Rec}} = \frac{\ln 2}{(t_{1/2})} \times \frac{V}{M_{\text{P450}}} \quad (2)$$

$$\text{CL}_{\text{int,HLM}} = \frac{\ln 2}{(t_{1/2})} \times \frac{V}{P_{\text{HLM}}} \quad (3)$$

RESULTS

Ritonavir and Lopinavir Inhibition of CYP3A7 DHEA-S 16 α -Hydroxylation. Kinetic parameters for the metabolism of DHEA-S to its 16 α -hydroxy metabolite by recombinant CYP3A7 Supersomes were determined based on a direct and sensitive LC-MS/MS analytical assay. Under our steady state assay conditions, the kinetic data (Figure 2) were fit to the Michaelis–Menten equation, and we obtained a K_m of 5.44 μM and a V_{max} of 9.40 nmol/min/nmol P450. The fit of the 16 α -hydroxy DHEA-S metabolite formation data was also assessed using the Hill equation, which provided comparable kinetic parameters to the Michaelis–Menten fit (Table S1).

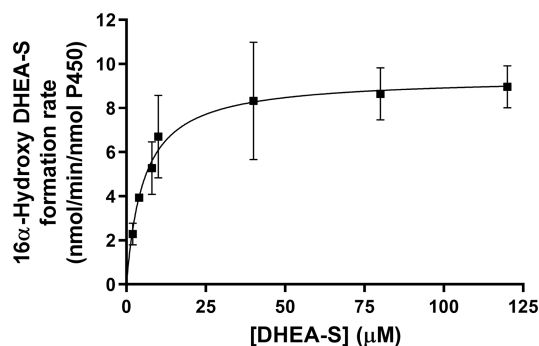


Figure 2. Kinetics of DHEA-S 16 α -hydroxylation by the recombinant CYP3A7 enzyme. DHEA-S 16 α -hydroxylation by CYP3A7 Supersomes fitted using the Michaelis–Menten equation, obtaining a K_m of 5.44 μM and a V_{max} of 9.40 nmol/min/nmol P450. Each data point represents the average of triplicate measurements, with error bars representing the standard deviations. The coefficient of determination, R^2 , for the regression model fit of DHEA-S metabolism kinetics was 0.986.

The *in vitro* inhibitory potency of lopinavir and ritonavir was then assessed for CYP3A7 DHEA-S 16 α -hydroxylation by determination of their respective IC₅₀ values, the protease inhibitor concentrations leading to 50% enzyme inhibition. DHEA-S, at the K_m concentration of 5 μ M, was incubated with the recombinant CYP3A7 enzyme and different concentration ranges of lopinavir (Figure 3) or ritonavir (Figure 4). An IC₅₀

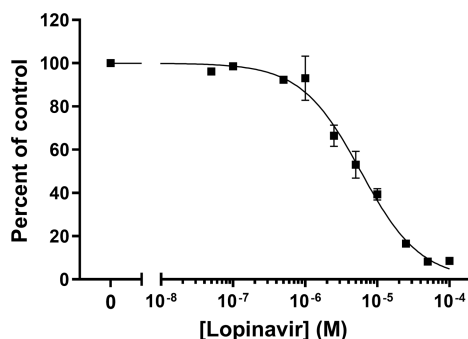


Figure 3. Lopinavir IC₅₀ for DHEA-S 16 α -hydroxylation by recombinant CYP3A7 enzyme. Each data point represents the average of triplicate measurements with error bars representing standard deviations, except for the 10⁻⁷ M data point which represents the average of only duplicate measurements (no standard deviation bar shown for that data point). The coefficient of determination, R^2 , for the regression model fit of lopinavir inhibition was 0.993. The IC₅₀ value for lopinavir was 5.88 μ M.

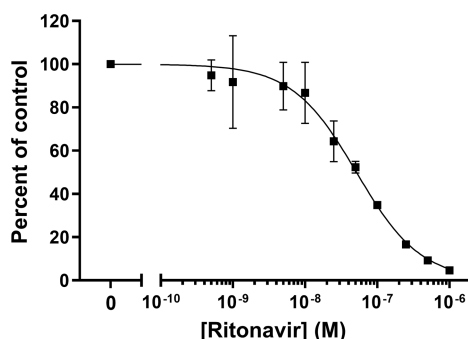


Figure 4. Ritonavir IC₅₀ for DHEA-S 16 α -hydroxylation by recombinant CYP3A7 enzyme. Each data point represents the average of triplicate measurements with error bars representing standard deviations. The coefficient of determination, R^2 , for the regression model fit of ritonavir inhibition was 0.994. The IC₅₀ value for ritonavir was 0.0514 μ M.

value of 5.88 μ M was estimated for lopinavir, and an IC₅₀ value of 0.0514 μ M was estimated for ritonavir, thus leading to a 110-fold difference in CYP3A7 inhibition potency between the two HIV protease inhibitors. CYP3A7 time-dependent inhibition was further assessed for ritonavir and DHEA-S 16 α -hydroxylation. Loss of CYP3A7 activity was measured as a function of time and ritonavir concentrations and by applying a 10-fold dilution to the preincubation samples (Figure 5). The decrease in activity of the recombinant CYP3A7 enzyme was preincubation time-dependent and concentration-dependent for ritonavir (Figure 5A). The derived k_{obs} values with the corresponding ritonavir concentrations (Figure 5B) allowed the estimation of the following kinetic inactivation constants: a k_{inact} value of 0.119 min⁻¹ as the maximum rate of inactivation and a K_I of 0.392 μ M as the ritonavir concentration leading to

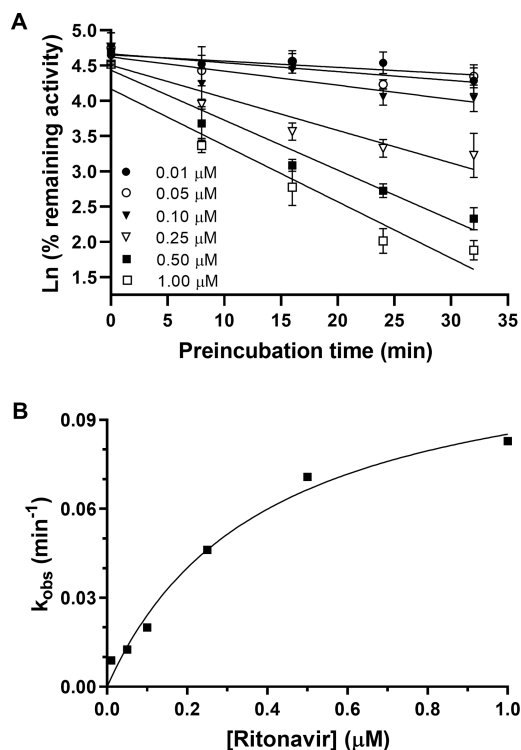


Figure 5. Time-dependent inhibition of CYP3A7 DHEA-S 16 α -hydroxylation by ritonavir. Pseudo-first-order kinetic plots (A) at six ritonavir concentrations based on the percent CYP3A7 remaining activity versus the preincubation time which led to the nonlinear regression fit (B) of the inactivation rate constants (k_{obs}) at the six ritonavir concentrations assessed. The K_I was determined to be 0.392 μ M, and the k_{inact} was determined to be 0.119 min⁻¹.

50% maximal inactivation. As a result, an inhibition rate constant, k_{inact}/K_I , of 0.304 min⁻¹· μ M⁻¹ was determined.

Inhibition of DHEA-S Metabolism by Lopinavir and Ritonavir in Neonatal Human Liver Microsomes. To assess the impact of the HIV protease inhibitors, lopinavir and ritonavir, on the metabolism of the endogenous androstane steroid DHEA-S by neonatal HLMs, DHEA-S was incubated in the presence of 8 μ M lopinavir without and with 0.5 μ M ritonavir (Figure 6). Solvent control incubations were carried out in parallel to establish the formation rate of the 16 α -hydroxy DHEA-S metabolite by neonatal HLMs. The formation rate of the 16 α -hydroxy DHEA-S in neonatal HLMs was determined as 2.08 nmol/min/mg protein for the solvent control, 1.19 nmol/min/mg protein with lopinavir, and 0.291 nmol/min/mg protein with lopinavir plus ritonavir. According to the change in the formation rate of the 16 α -hydroxy DHEA-S metabolite over the 30 min incubation, lopinavir inhibited the formation of the hydroxy metabolite by 41%, and lopinavir plus ritonavir inhibited metabolite formation by 86% in the neonatal HLMs.

Lopinavir Clearance by Recombinant CYP3A4 and CYP3A7 Enzymes. Lopinavir clearance by recombinant CYP3A4 and CYP3A7 enzymes was initially assessed with 2 pmol CYP enzyme/mL and with normalization of the protein content using the Supersomes insect cell control microsomes. After a 50 min incubation, the mean lopinavir percent loss was over 80% for CYP3A4 Supersomes and less than 10% for CYP3A7 Supersomes. The *in vitro* half-life ($t_{1/2}$) and intrinsic clearance ($CL_{int,Rec}$) for lopinavir were determined for the

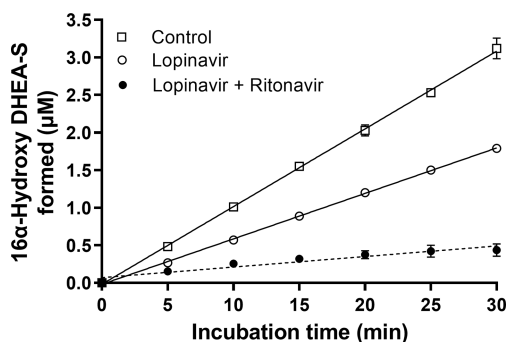


Figure 6. Effect of lopinavir and ritonavir on DHEA-S hydroxylation by neonatal human liver microsomes. Pooled neonatal human liver microsomes (0.05 mg/mL) were incubated with DHEA-S (50 μ M) in the presence of lopinavir and ritonavir to assess formation *in vitro* of the 16 α -hydroxy DHEA-S metabolite. Each data point represents the average of triplicate measurements with error bars representing standard deviations. The formation rate of the 16 α -hydroxy DHEA-S in neonatal HLMs was determined as 2.08 nmol/min/mg protein for the solvent control, 1.19 nmol/min/mg protein with lopinavir, and 0.291 nmol/min/mg protein with lopinavir plus ritonavir.

recombinant CYP3A4 based on the slope of the linear fit for the natural logarithm of the percent remaining over time (Figure 7). The lopinavir *in vitro* half-life and intrinsic

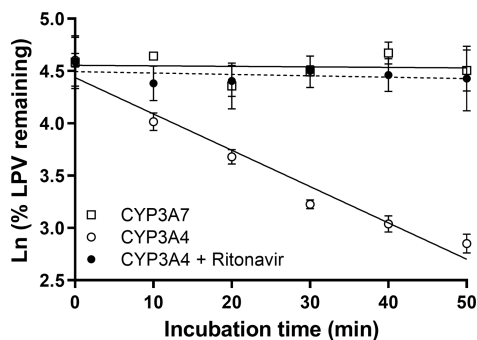


Figure 7. Lopinavir intrinsic clearance by recombinant CYP3A4 and CYP3A7 enzymes. CYP3A Supersomes (2 pmol/mL) were incubated with lopinavir (1 μ M) to assess the *in vitro* half-life and intrinsic clearance rate. The effect of ritonavir on lopinavir clearance by CYP3A4 was assessed at 0.0625 μ M. Each data point represents the average of triplicate measurements with error bars representing standard deviations.

clearance rate for the recombinant CYP3A4 were 20.0 min and 17.4 μ L/min-pmol, respectively (Table 1). In contrast, when the inhibitor ritonavir was present (at a 16-fold lower concentration than lopinavir³³), the lopinavir percent loss by the recombinant CYP3A4 was less than 15%. This low

metabolic clearance expected for the CYP3A4 Supersomes incubated in the presence of ritonavir was, in fact, comparable to the clearance observed with the CYP3A7 Supersomes only. A substrate loss of 20% or less is in the range of the analytical variability and did not allow the establishment of the *in vitro* half-life and intrinsic clearance rate for CYP3A7 under these conditions. To circumvent the limitation of the assay, lopinavir clearance was assessed in the presence of 40 pmol P450 enzyme/mL of the recombinant CYP3A7 (Figure S1). After a 50 min incubation, a mean lopinavir percent loss of 63.4% was measured for CYP3A7 Supersomes. The lopinavir *in vitro* half-life and intrinsic clearance rate were then determined for the recombinant CYP3A7 as 31.2 min and 0.555 μ L/min-pmol, respectively (Table 1). When comparing the lopinavir intrinsic clearance rate of the recombinant CYP3A4 and CYP3A7, a 31-fold lower rate was observed for the CYP3A7 enzyme.

Lopinavir Clearance by Neonatal and Adult Human Liver Microsomes. Lopinavir clearance by adult and neonatal HLMs was assessed using 0.02 mg HLM protein/mL. After a 30 min incubation, the mean lopinavir percent loss was about 94% for the adult HLMs and 21% for the neonatal HLMs. The *in vitro* half-life ($t_{1/2}$) and intrinsic clearance ($CL_{int,HLM}$) for lopinavir were determined for the adult HLMs based on the slope of the linear fit for the natural logarithm of the percent remaining over time (Figure 8). The lopinavir *in vitro* half-life

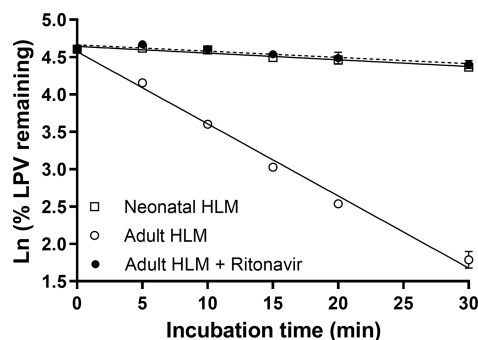


Figure 8. Lopinavir intrinsic clearance by adult and neonatal human liver microsomes. Human liver microsomes (0.02 mg/mL) were incubated with lopinavir (1 μ M) to assess the *in vitro* half-life and intrinsic clearance rate. The effect of ritonavir on lopinavir clearance by adult human liver microsomes was assessed at 0.0625 μ M. Each data point represents the average of triplicate measurements with error bars representing standard deviations.

and intrinsic clearance rate for the adult HLMs were estimated as 7.18 min and 4830 μ L/min-mg, respectively. When the inhibitor ritonavir (62.5 nM) was added to the adult HLM incubation, the lopinavir loss was less than 20% and thus comparable to the limited clearance observed with neonatal

Table 1. Lopinavir Intrinsic Clearance Data for Recombinant CYP3A4 and CYP3A7 Supersomes and Adult and Neonatal Human Liver Microsomes

test system	test system concentration	slope	$t_{1/2}^a$ (min)	CL_{int}^b	
				(μ L/min-pmol)	(μ L/min-mg)
recombinant CYP enzymes	CYP3A4 Supersomes	2 pmol/mL	20.0	17.4	
	CYP3A7 Supersomes	40 pmol/mL	31.2	0.555	
human liver microsomes	pooled adult HLMs	0.02 mg/mL	7.18		4830
	pooled neonatal HLMs	0.1 mg/mL	52.1		133

^a $t_{1/2}$, *in vitro* half-life. ^b CL_{int} , intrinsic clearance.

HLMs. Due to the limited substrate loss observed with the neonatal HLM at 0.02 mg/mL, lopinavir clearance measurements were done in the presence of 0.1 mg/mL neonatal HLMs (Figure S2). After a 30 min incubation, a mean lopinavir percent loss of 32% was measured with the neonatal HLMs. The lopinavir *in vitro* half-life and intrinsic clearance were determined for the neonatal HLMs as 52.1 min and 133 $\mu\text{L}/\text{min}\cdot\text{mg}$, respectively (Table 1). When comparing the lopinavir intrinsic clearance rate of the adult and neonatal HLMs, a 36-fold lower rate was observed for the neonatal HLMs.

DISCUSSION

The use of ritonavir-boosted lopinavir as a prophylactic ARV treatment for pregnant women and neonates has been assessed in several clinical settings, uncovering adrenal hormonal imbalance and leading, in some cases, to transient adrenal dysfunction, in particular, for preterm and previously *in utero* exposed infants.^{7,8,13} Abnormal plasma levels of 17-OHP, DHEA, and DHEA-S have been measured in neonates receiving the protease inhibitor combination with mean increases of about 3-, 5-, and 20-fold the normal values, respectively.^{7,8} The ritonavir-boosted lopinavir regimen has been well characterized in adults, with both drugs acting as substrates and inhibitors of the CYP3A enzymes.^{11,15,16,38,39} However, understanding the effect of this ARV regimen on the metabolism of the endogenous androstane steroid hormone DHEA-S by the hepatic CYP3A7, the predominant cytochrome P450 enzyme in the fetal and neonatal liver, necessitated our scientific consideration. Interestingly, during the fetal period, the 16 α -hydroxylation of DHEA-S by CYP3A7 is thought to be important in controlling placental estriol synthesis and full-term gestation.^{26–28} During the neonatal phase, CYP3A7 activity, maximal at birth, starts to decline after the first week of life, progressively switching to the CYP3A4 isoform throughout the first year.^{20–23} Despite the changes in expression and activity level, CYP3A7 is the major CYP3A isoform in the neonatal liver and is thought to be important in both drug and steroid metabolism processes.^{18,22,23} Inhibition of CYP3A7 by protease inhibitors has been previously assessed *in vitro* using testosterone as the probe substrate, and it revealed ritonavir as a potent inhibitor with an IC_{50} of 0.6 μM .¹⁶ Although the CYP3A isoforms overlap in substrate specificity, these enzymes have different kinetic properties depending on the substrate.^{25,40} CYP3A7 is often considered to be a less metabolically active isoform, but in the case of the androstane hormones, DHEA and DHEA-S, CYP3A7 has demonstrated higher reaction velocities (V_{max}) and affinities (K_{m}) than CYP3A4.²⁵ In this study, we evaluated the *in vitro* inhibition potency of lopinavir and ritonavir for CYP3A7 DHEA-S 16 α -hydroxylation using the recombinant enzyme and determined an IC_{50} of 0.0514 μM for ritonavir, about 10-fold higher inhibition potency than for testosterone 6 β -hydroxylation. Lopinavir was a 100-fold less potent CYP3A7 inhibitor with an IC_{50} of 5.88 μM for DHEA-S 16 α -hydroxylation. Furthermore, ritonavir has been identified as a potent mechanism-based inactivator (MBI) of CYP3A4 and CYP3A5,³⁴ but no evaluation of it as an MBI has yet been done for the CYP3A7 isoform. Here, we demonstrated for the first time that ritonavir was a potent time-dependent inhibitor (TDI) of CYP3A7 with a K_{I} of 0.392 μM and an inhibition rate constant of 0.304 $\text{min}^{-1}\cdot\mu\text{M}^{-1}$. The K_{I} and inhibition rate constant were about 4- and 10-fold lower, respectively,

compared to ritonavir inhibition of CYP3A4 testosterone 6 β -hydroxylation.³⁴ TDI is considered as a (quasi-) irreversible type of enzyme inhibition, and thus, it could have a persistent effect on CYP3A7 activity in neonates since only *de novo* synthesis of the enzyme would overcome the time-dependent inhibition after the treatment is discontinued. This could lead to further risks for drug–drug interactions and metabolic insufficiencies in the treated neonates. To further understand the impact of lopinavir and ritonavir inhibition on endogenous CYP3A7 metabolic activity, formation of the 16 α -hydroxy DHEA-S metabolite was monitored in neonatal pooled human liver microsomes in the absence and presence of lopinavir and lopinavir plus ritonavir. Both protease inhibitors were tested at clinically relevant concentrations in the presence of a saturating concentration of DHEA-S. The concentration of DHEA-S (50 μM) used for the neonatal pooled human liver microsome inhibition assessment is apropos according to the study by Simon et al. in 2011 observing an increase in the median plasma concentration of DHEA-S in ritonavir-boosted lopinavir term newborns to 25.1 μM (with an interquartile range of 3.7–70.5 μM). For lopinavir, the concentration used was near the C_{max} reported by Foissac et al. in 2017, and ritonavir was about 16-fold lower than the lopinavir concentration, as reported in the Kaletra package insert.^{32,33} Our measurement indicated that lopinavir plus ritonavir was nearly completely inhibiting the metabolism of DHEA-S to its 16 α -hydroxyl derivative in neonatal human liver microsomes.

The mechanism leading to the adrenal hormone imbalance observed in neonates receiving ritonavir-boosted lopinavir is not well understood. Kariyawasam et al. proposed in 2020 that the inhibition of two adrenal cytochrome P450 enzymes, CYP21A2 and CYP17A1, by lopinavir may result in the adrenal hormonal changes.¹³ Effectively, mutations in the CYP21A2 gene triggering deficiency in 21-hydroxylase activity (21OHD) is a common cause for congenital adrenal hyperplasia (CAH).⁴¹ In 21OHD, production of cortisol and aldosterone is impaired and necessitates corticosteroid replacement therapy. The deficiency in cortisol triggers corticotropin (ACTH) synthesis by disruption of the cortisol negative feedback loop which stimulates production by the adrenal glands of cortisol precursors (e.g., 17-OHP). These precursors are then shunted toward excess production of androgenic hormones, as seen in neonates receiving the lopinavir-ritonavir treatment. In the case of the CYP17A1 enzyme, mutations resulting in 17-hydroxylase/17-20-lyase deficiency, a rare condition linked to congenital adrenal hyperplasia, alter synthesis of cortisol and production of androgenic hormones.⁴² Deficiency in the adrenal enzymatic activity of CYP17A1 results in low levels of DHEA and DHEA-S which would be inconsistent with the biochemical hormonal signature observed in neonates receiving the protease inhibitor combination. Simon et al. in 2011 released data about twin preterm infants that were exposed *in utero* to lopinavir-ritonavir combination and received the same PI treatment from birth.⁷ Both neonates presented symptoms of adrenal insufficiency with severe electrolytic disorders after the PI treatment started. Interestingly, the twins had normal values for 17OHP but extremely elevated blood levels of DHEA-S. The normal values of 17OHP would conflict with an impairment of CYP21A2 activity. However, these biochemical data would be consistent with impairment of DHEA-S metabolism. Thus, here we are proposing an alternative mechanism for the adrenal hormonal imbalance observed in neonates treated with ritonavir-boosted

lopinavir entailing the inhibition of CYP3A7 by ritonavir (and to a lesser extent lopinavir) that would hinder DHEA-S (and DHEA) metabolism and cause accumulation of the androgen hormone(s) and their precursors. This alternative mechanism is in agreement with the study by Kariyawasam et al. in 2014 where neonates receiving the ritonavir-boosted lopinavir had normal cortisol levels before and after ACTH stimulation (conflicting with CYP21A2 involvement), whereas 17-OHP, DHEA, and DHEA-S plasma levels were elevated.⁸ An interesting case report was published regarding a 10-day-old full-term neonate who, after receiving an ARV combinatorial treatment of two NRTIs and the NNRTI nevirapine, presented severe symptoms of lethargy and respiratory distress.⁹ The adrenal hormonal profile of the neonate was abnormal with elevated levels of 17-OHP, DHEA-S, androstenedione, and aldosterone. Although nevirapine is a known substrate, inhibitor, and inducer of CYP3A4 in adults, limited information is available about nevirapine effects on CYP3A7 in neonates.^{43–45} Recent work in our laboratory has indicated the potential for nevirapine to inhibit CYP3A7 (data not shown). Therefore, inhibition of CYP3A7 by ritonavir-lopinavir or nevirapine could suggest a common mode of action of these drugs hindering DHEA and DHEA-S metabolism in the neonatal liver and leading to an increase in circulating concentrations of these androgenic hormones and their precursors. It is notable that the neonates presenting adrenal hormonal imbalance after receiving the ARV treatment generally returned to normal levels a few days after stopping the treatment.^{7–9} The early postnatal period is a transitional phase for the adrenal glands undergoing important structural remodeling with rapid involution of the inner fetal zone, the region of the adrenal cortex producing a large quantity of androgens that are essential for fetal development.⁴⁶ With the involution of the fetal zone, DHEA-S production by the adrenal is decreased, and the zona glomerulosa and fasciculata are rapidly developing. This maturation process is gestational age-dependent and can have profound effects on preterm infants and their survival rate.^{47,48} Interestingly, the hepatic activity of CYP3A7 mirrors the adrenal DHEA-S production during the fetal and neonatal periods,^{23,49} both increasing throughout the fetal life and reaching maximal level at birth only then to decrease rapidly over the first few weeks of life. This suggests an essential role for the hepatic CYP3A7 enzyme for controlling DHEA-S plasma concentration via metabolism during the pre- and postnatal periods and, hence, maintaining the cortisol/DHEA(-S) ratio.^{50,51}

Neonates are a fragile population for which the mechanisms of absorption, distribution, metabolism, and elimination (ADME) of drugs are understudied and the dosing of drugs is largely extrapolated from adult data using weight adjustment and allometric scaling factors.^{52,53} Only limited ADME data have been obtained for neonates receiving the ritonavir-boosted lopinavir regimen as a prophylactic ARV treatment.^{32,54–56} In adults, lopinavir, like other protease inhibitors, is rapidly metabolized by the liver through the CYP3A4 pathway, and therefore, dosing requires the addition of the pharmacokinetic enhancer ritonavir, a potent CYP3A4 inhibitor.³⁰ The neonatal period is a time where many developmental changes occur, including those taking place in the liver.^{57,58} As previously mentioned, CYP3A7 is the major cytochrome P450 in the neonatal liver and is considered to have the lowest metabolizing activity among the CYP3A isoforms.⁴⁰ To understand the efficiency of CYP3A7 to

metabolize lopinavir, we investigated the clearance of lopinavir using the recombinant CYP3A7 enzyme and compared it to the CYP3A4 isoform. Lopinavir clearance by CYP3A7 was characterized by a low intrinsic clearance rate equivalent to CYP3A4 incubated with the inhibitor ritonavir. Effectively, a difference of over 30-fold was measured for lopinavir clearance between CYP3A4 and CYP3A7. When assessing the intrinsic clearance rate for neonatal pooled HLMs, we also measured a low metabolic rate for lopinavir metabolism, analogous to the adult HLMs incubated with ritonavir. This study illustrates the differences in metabolic potential between the adult and neonatal liver which needs to be taken into consideration before dosing drugs in this fragile patient population. Our data specifically raise the question for the need of the pharmacological enhancer ritonavir with the lopinavir treatment of neonates, at least until the hepatic expression of CYP3A4 is high enough to impact clearance of the protease inhibitor. Currently, more studies are required to obtain a comprehensive understanding of the temporal expression of the CYP3A isoforms in the liver of the developing infant, especially during the first 6 months of life, and to estimate the individual variability in expression of these important enzymes and their impact on drug metabolism. As a potent TDI of CYP3A7, ritonavir may further hinder the clearance of lopinavir by the neonatal liver, potentially causing it to accumulate to a toxic level.¹²

In 2011, the Food and Drug Administration (FDA) issued a drug safety warning for the Kaletra formulation not recommending the drug for infants <14 days of age (or preterm babies <42 weeks postmenstrual age) due to increased risks for metabolic and cardiac toxicities, including transient symptomatic adrenal insufficiency.¹² Although the toxicities observed in neonates may be associated with some of the inactive ingredients (propylene glycol and ethanol), our data suggest that ritonavir, a potent CYP3A7 time-dependent inhibitor, has a profound impact on lopinavir clearance (being more slowly metabolized by neonatal than adult HLMs) and on metabolism of the endogenous androgenic hormone DHEA-S. The requirement of this pharmacokinetic enhancer for lopinavir prophylactic ARV treatment of neonates should be carefully reassessed.

■ ASSOCIATED CONTENT

SI Supporting Information

The Supporting Information is available free of charge at <https://pubs.acs.org/doi/10.1021/acs.chemrestox.1c00028>.

Michaelis–Menten and Hill fit comparison for recombinant CYP3A7 DHEA-S kinetics and lopinavir clearance data for recombinant CYP3A7 enzyme and neonatal HLMs (PDF)

■ AUTHOR INFORMATION

Corresponding Author

Jed N. Lampe – Department of Pharmaceutical Sciences, Skaggs School of Pharmacy, University of Colorado, Aurora, Colorado 80045, United States; orcid.org/0000-0003-0794-2263; Phone: (303) 724-3397; Email: jed.lampe@cuanschutz.edu; Fax: (303) 724-7266

Author

Sylvie E. Kandel – Department of Pharmaceutical Sciences, Skaggs School of Pharmacy, University of Colorado, Aurora,

Colorado 80045, United States;  orcid.org/0000-0002-8059-8035

Complete contact information is available at:
<https://pubs.acs.org/10.1021/acs.chemrestox.1c00028>

Author Contributions

J.N.L. and S.E.K. participated in research design and wrote the manuscript. S.E.K. conducted experiments and performed data analysis.

Funding

The research reported here was supported by the National Institutes of Health, National Institute of Allergy and Infectious Diseases (NIAID) Award Number R01AI150494 (J.N.L.).

Notes

The content is solely the responsibility of the authors and does not necessarily represent the official views of the National Institutes of Health.

The authors declare no competing financial interest.

ACKNOWLEDGMENTS

Our special acknowledgments are extended to the Liver Center of the University of Kansas, Medical Center (Kansas City, KS) and Ms. Kelsey Strube for the donations of neonatal liver tissues.

ABBREVIATIONS

16 α -hydroxy DHEA-S, 16 α -hydroxydehydroepiandrosterone 3-sulfate; 17-OHP, 17 α -hydroxyprogesterone; 21-OHD, 21-hydroxylase deficiency; ACTH, adrenocorticotropic hormone; ADME, absorption, distribution, metabolism, and elimination; ART, antiretroviral therapy; ARV, antiretroviral; BCA, bichinchoninic acid; CAH, congenital adrenal hyperplasia; CE, collision energy; CL_{int} , intrinsic clearance; $CL_{int,HLM}$, intrinsic clearance for HLMs; $CL_{int,CYP}$, intrinsic clearance for recombinant CYP; C_{max} , maximum plasma concentration; CV, cone voltage; CYP, cytochrome P450; DHEA, dehydroepiandrosterone; DHEA-S, dehydroepiandrosterone 3-sulfate; DHEA-S- d_5 , dehydroepiandrosterone- d_5 -3-sulfate; EDTA, ethylenediaminetetraacetic acid; FDA, Food and Drug Administration; HIV, human immunodeficiency virus; HLMs, human liver microsomes; HPLC, high performance liquid chromatography; INSTI(s), integrase strand transcriptase inhibitor(s); k , elimination rate constant; k_{obs} , observed inactivation rate constant; LC-MS/MS, liquid chromatography tandem mass spectrometry; LPV, lopinavir; MBI, mechanism-based inactivator; M_{P450} , moles of CYP enzyme; MRM, multiple reaction monitoring; MS, mass spectrometry; NADP⁺, β -nicotinamide adenine dinucleotide phosphate; NADPH, β -nicotinamide adenine dinucleotide phosphate reduced; NNRTI(s), non-nucleoside reverse transcriptase inhibitor(s); NRTI(s), nucleoside reverse transcriptase inhibitor(s); PI(s), protease inhibitor(s); $t_{1/2}$, *in vitro* half-life; TDI, time-dependent inhibitor; UPLC, ultra-performance liquid chromatography; V , incubation volume

REFERENCES

(1) Newell, M. L. (2001) Prevention of mother-to-child transmission of HIV: challenges for the current decade. *Bull. World Health Organ* 79 (12), 1138–44.

(2) Lumaca, A., Galli, L., de Martino, M., and Chiappini, E. (2018) Paediatric HIV-1 infection: updated strategies of prevention mother-to-child transmission. *J. Chemother.* 30 (4), 193–202.

(3) United Nations Children's Fund. (2020) Elimination of mother-to-child transmission: progress in reducing new HIV infections among children, but not fast enough to save lives. Available from <https://data.unicef.org/topic/hiv/aids/emtct/> (accessed 2021-04-01).

(4) World Health Organization. (2010) Antiretroviral drugs for treating pregnant women and preventing HIV infection in infants. Recommendations for a public health approach. Available from <https://www.who.int/hiv/pub/mtct/antiretroviral2010/en/> (accessed 2021-04-01).

(5) World Health Organization. (2019) Update of recommendations on first- and second-line antiretroviral regimens. Available from <https://www.who.int/hiv/pub/arv/arv-update-2019-policy/en/> (accessed 2021-04-01).

(6) Kirmse, B., Baumgart, S., and Rakhmanina, N. (2013) Metabolic and mitochondrial effects of antiretroviral drug exposure in pregnancy and postpartum: implications for fetal and future health. *Semin Fetal Neonatal Med.* 18 (1), 48–55.

(7) Simon, A., Warszawski, J., Kariyawasam, D., Le Chenadec, J., Benhammou, V., Czernichow, P., Foissac, F., Laborde, K., Tréluyer, J. M., Firtion, G., Layouni, I., Munzer, M., Bavoux, F., Polak, M., and Blanche, S. (2011) Association of prenatal and postnatal exposure to lopinavir-ritonavir and adrenal dysfunction among uninfected infants of HIV-infected mothers. *Jama* 306 (1), 70–8.

(8) Kariyawasam, D., Simon, A., Laborde, K., Parat, S., Souchon, P. F., Frange, P., Blanche, S., and Polak, M. (2014) Adrenal enzyme impairment in neonates and adolescents treated with ritonavir and protease inhibitors for HIV exposure or infection. *Horm. Res. Paediatr.* 81 (4), 226–31.

(9) Eng, L., Raisingani, M., Kaul, A., Mehta, S., Prasad, K., David, R., and Shah, B. (2018) Severe metabolic disturbance in an human immunodeficiency virus-exposed newborn: Possible effect of *in utero* antiretroviral exposure. *Journal of Clinical Neonatology* 7 (3), 158–161.

(10) Sibiude, J., Warszawski, J., Tubiana, R., Dollfus, C., Faye, A., Rouzioux, C., Teglas, J. P., Ekoukou, D., Blanche, S., and Mandelbrot, L. (2012) Premature delivery in HIV-infected women starting protease inhibitor therapy during pregnancy: role of the ritonavir boost? *Clin. Infect. Dis.* 54 (9), 1348–60.

(11) Corbett, A. H., Lim, M. L., and Kashuba, A. D. (2002) Kaletra (lopinavir/ritonavir). *Ann. Pharmacother.* 36 (7–8), 1193–203.

(12) U.S. Food and Drug Administration. (2011) FDA drug Safety communication: Serious health problems seen in premature babies given Kaletra (lopinavir/ritonavir) oral solution (updated 2017 August 4th). Available from www.fda.gov/drugs/drugsafety/ucm246002.htm (accessed 2021-04-01).

(13) Kariyawasam, D., Peries, M., Foissac, F., Eymard-Duvernay, S., Tylleskär, T., Singata-Madliki, M., Kankasa, C., Meda, N., Tumwine, J., Mwiya, M., Engebretsen, I., Flück, C. E., Hartmann, M. F., Wudy, S. A., Hirt, D., Tréluyer, J. M., Molès, J. P., Blanche, S., Van De Perre, P., Polak, M., and Nagot, N. (2020) Lopinavir-ritonavir impairs adrenal function in infants. *Clin Infect Dis* 71 (4), 1030–1039.

(14) Fish, K. J., Rice, S. A., and Margary, J. (1988) Contrasting effects of etomidate and propylene glycol upon enflurane metabolism and adrenal steroidogenesis in Fischer 344 rats. *Anesthesiology* 68 (2), 189–93.

(15) Kumar, G. N., Dykstra, J., Roberts, E. M., Jayanti, V. K., Hickman, D., Uchic, J., Yao, Y., Surber, B., Thomas, S., and Granneman, G. R. (1999) Potent inhibition of the cytochrome P-450 3A-mediated human liver microsomal metabolism of a novel HIV protease inhibitor by ritonavir: A positive drug-drug interaction. *Drug Metab. Dispos.* 27 (8), 902–8.

(16) Granfors, M. T., Wang, J. S., Kajosaari, L. I., Laitila, J., Neuvonen, P. J., and Backman, J. T. (2006) Differential inhibition of cytochrome P450 3A4, 3A5 and 3A7 by five human immunodeficiency virus (HIV) protease inhibitors *in vitro*. *Basic Clin. Pharmacol. Toxicol.* 98 (1), 79–85.

- (17) Hossain, M. A., Tran, T., Chen, T., Mikus, G., and Greenblatt, D. J. (2017) Inhibition of human cytochromes P450 *in vitro* by ritonavir and cobicistat. *J. Pharm. Pharmacol.* 69 (12), 1786–1793.
- (18) Li, H., and Lampe, J. N. (2019) Neonatal cytochrome P450 CYP3A7: A comprehensive review of its role in development, disease, and xenobiotic metabolism. *Arch. Biochem. Biophys.* 673, 108078.
- (19) Ortiz de Montellano, P. R. (2005) *Cytochrome P450: Structure, Mechanism, and Biochemistry*, 3rd ed., Kluwer Academic/Plenum Publishers, New York, DOI: 10.1007/b139087.
- (20) Lacroix, D., Sonnier, M., Moncion, A., Cheron, G., and Cresteil, T. (1997) Expression of CYP3A in the human liver – Evidence that the shift between CYP3A7 and CYP3A4 occurs immediately after birth. *Eur. J. Biochem.* 247 (2), 625–34.
- (21) de Wildt, S. N., Kearns, G. L., Leeder, J. S., and van den Anker, J. N. (1999) Cytochrome P450 3A: ontogeny and drug disposition. *Clin. Pharmacokinet.* 37 (6), 485–505.
- (22) Hines, R. N. (2007) Ontogeny of human hepatic cytochromes P450. *J. Biochem. Mol. Toxicol.* 21 (4), 169–75.
- (23) Lu, H., and Rosenbaum, S. (2014) Developmental pharmacokinetics in pediatric populations. *J. Pediatr Pharmacol Ther* 19 (4), 262–76.
- (24) Kitada, M., Kamataki, T., Itahashi, K., Rikihisa, T., and Kanakubo, Y. (1987) P-450 HFLa, a form of cytochrome P-450 purified from human fetal livers, is the 16 alpha-hydroxylase of dehydroepiandrosterone 3-sulfate. *J. Biol. Chem.* 262 (28), 13534–7.
- (25) Torimoto, N., Ishii, I., Toyama, K., Hata, M., Tanaka, K., Shimomura, H., Nakamura, H., Ariyoshi, N., Ohmori, S., and Kitada, M. (2007) Helices F-G are important for the substrate specificities of CYP3A7. *Drug Metab. Dispos.* 35 (3), 484–92.
- (26) Kaludjerovic, J., and Ward, W. E. (2012) The Interplay between Estrogen and Fetal Adrenal Cortex. *J. Nutr. Metab.* 2012, 837901.
- (27) Chatuphonprasert, W., Jarukamjorn, K., and Ellinger, I. (2018) Physiology and Pathophysiology of Steroid Biosynthesis, Transport and Metabolism in the Human Placenta. *Front. Pharmacol.* 9, 1027.
- (28) Schleifer, R. A., Bradley, L. A., Richards, D. S., and Ponting, N. R. (1995) Pregnancy outcome for women with very low levels of maternal serum unconjugated estriol on second-trimester screening. *Am. J. Obstet. Gynecol.* 173 (4), 1152–6.
- (29) Reynolds, J. W., Turnipseed, M. R., and Mirkin, B. L. (1975) Adrenal cortical function in abnormal newborn infants. *J. Steroid Biochem.* 6 (5), 669–72.
- (30) Kempf, D. J., Marsh, K. C., Kumar, G., Rodrigues, A. D., Denissen, J. F., McDonald, E., Kukulka, M. J., Hsu, A., Granneman, G. R., Baroldi, P. A., Sun, E., Pizzuti, D., Plattner, J. J., Norbeck, D. W., and Leonard, J. M. (1997) Pharmacokinetic enhancement of inhibitors of the human immunodeficiency virus protease by coadministration with ritonavir. *Antimicrob. Agents Chemother.* 41 (3), 654–60.
- (31) Pearce, R. E., McIntyre, C. J., Madan, A., Sanzgiri, U., Draper, A. J., Bullock, P. L., Cook, D. C., Burton, L. A., Latham, J., Nevins, C., and Parkinson, A. (1996) Effects of freezing, thawing, and storing human liver microsomes on cytochrome P450 activity. *Arch. Biochem. Biophys.* 331 (2), 145–69.
- (32) Foissac, F., Blume, J., Tréluyer, J. M., Tylleskär, T., Kankasa, C., Meda, N., Tumwine, J. K., Singata-Madliki, M., Harper, K., Illamola, S. M., Bouazza, N., Nagot, N., Van de Perre, P., Blanche, S., and Hirt, D. (2017) Are Prophylactic and Therapeutic Target Concentrations Different?: the Case of Lopinavir-Ritonavir or Lamivudine Administered to Infants for Prevention of Mother-to-Child HIV-1 Transmission during Breastfeeding. *Antimicrob. Agents Chemother.* 61 (2), e01869-16.
- (33) KALETRA package insert (revision November 2016). Available from https://www.accessdata.fda.gov/drugsatfda_docs/label/2016/021251s052_021906s0461bl.pdf (accessed 2021-04-01).
- (34) Ernest, C. S., 2nd, Hall, S. D., and Jones, D. R. (2005) Mechanism-based inactivation of CYP3A by HIV protease inhibitors. *J. Pharmacol. Exp. Ther.* 312 (2), 583–91.
- (35) Burt, H. J., Pertinez, H., Säll, C., Collins, C., Hyland, R., Houston, J. B., and Galetin, A. (2012) Progress curve mechanistic modeling approach for assessing time-dependent inhibition of CYP3A4. *Drug Metab. Dispos.* 40 (9), 1658–67.
- (36) Nagar, S., Jones, J. P., and Korzekwa, K. (2014) A numerical method for analysis of *in vitro* time-dependent inhibition data. Part 1. *Drug Metab. Dispos.* 42 (9), 1575–86.
- (37) Korzekwa, K., Tweedie, D., Argikar, U. A., Whitcher-Johnstone, A., Bell, L., Bickford, S., and Nagar, S. (2014) A numerical method for analysis of *in vitro* time-dependent inhibition data. Part 2. Application to experimental data. *Drug Metab. Dispos.* 42 (9), 1587–95.
- (38) Kumar, G. N., Rodrigues, A. D., Buko, A. M., and Denissen, J. F. (1996) Cytochrome P450-mediated metabolism of the HIV-1 protease inhibitor ritonavir (ABT-538) in human liver microsomes. *J. Pharmacol. Exp Ther* 277 (1), 423–31.
- (39) Kumar, G. N., Jayanti, V., Lee, R. D., Whittern, D. N., Uchic, J., Thomas, S., Johnson, P., Grabowski, B., Sham, H., Betebenner, D., Kempf, D. J., and Denissen, J. F. (1999) *In vitro* metabolism of the HIV-1 protease inhibitor ABT-378: species comparison and metabolite identification. *Drug Metab. Dispos.* 27 (1), 86–91.
- (40) Williams, J. A., Ring, B. J., Cantrell, V. E., Jones, D. R., Eckstein, J., Ruterbories, K., Hamman, M. A., Hall, S. D., and Wrighton, S. A. (2002) Comparative metabolic capabilities of CYP3A4, CYP3A5, and CYP3A7. *Drug Metab. Dispos.* 30 (8), 883–91.
- (41) Parsa, A. A., and New, M. I. (2017) Steroid 21-hydroxylase deficiency in congenital adrenal hyperplasia. *J. Steroid Biochem. Mol. Biol.* 165 (Pt A), 2–11.
- (42) Auchus, R. J. (2017) Steroid 17-hydroxylase and 17,20-lyase deficiencies, genetic and pharmacologic. *J. Steroid Biochem. Mol. Biol.* 165 (Pt A), 71–78.
- (43) Erickson, D. A., Mather, G., Trager, W. F., Levy, R. H., and Keirns, J. J. (1999) Characterization of the *in vitro* biotransformation of the HIV-1 reverse transcriptase inhibitor nevirapine by human hepatic cytochromes P-450. *Drug Metab. Dispos.* 27 (12), 1488–95.
- (44) Wen, B., Chen, Y., and Fitch, W. L. (2009) Metabolic activation of nevirapine in human liver microsomes: dehydrogenation and inactivation of cytochrome P450 3A4. *Drug Metab. Dispos.* 37 (7), 1557–62.
- (45) Lamson, M., MacGregor, T., Riska, P., Erickson, D., Maxfield, P., Rowland, L., Gigliotti, M., Robinson, P., Azzam, S., and Keirns, J. (1999) Nevirapine Induces Both CYP3A4 and CYP2B6 Metabolic Pathways. *Clin. Pharmacol. Ther.* 65 (2), 137–137.
- (46) Antonini, S. R., Stecchini, M. F., and Ramalho, F. S. (2020) Chapter 36 - Development and Function of the Adrenal Cortex and Medulla in the Fetus and Neonate. In *Maternal-Fetal and Neonatal Endocrinology* (Kovacs, C. S., and Deal, C. L., Eds.) pp 611–623, Academic Press.
- (47) Masumoto, K., Tagawa, N., Kobayashi, Y., and Kusuda, S. (2019) Cortisol production in preterm infants with or without late-onset adrenal insufficiency of prematurity: A prospective observational study. *Pediatrics & Neonatology* 60 (5), S04–S11.
- (48) Bolt, R. J., Van Weissenbruch, M. M., Popp-Snijders, C., Sweep, F. G., Lafeber, H. N., and Delemarre-van de Waal, H. A. (2002) Maturity of the adrenal cortex in very preterm infants is related to gestational age. *Pediatr. Res.* 52 (3), 405–10.
- (49) Rainey, W. E., Carr, B. R., Sasano, H., Suzuki, T., and Mason, J. I. (2002) Dissecting human adrenal androgen production. *Trends Endocrinol. Metab.* 13 (6), 234–9.
- (50) Buhimschi, C. S., Turan, O. M., Funai, E. F., Azpurua, H., Bahtiyar, M. O., Turan, S., Zhao, G., Dulay, A., Bhandari, V., Copel, J. A., and Buhimschi, I. A. (2008) Fetal adrenal gland volume and cortisol/dehydroepiandrosterone sulfate ratio in inflammation-associated preterm birth. *Obstet. Gynecol.* 111 (3), 715–22.
- (51) Kamin, H. S., and Kertes, D. A. (2017) Cortisol and DHEA in development and psychopathology. *Horm. Behav.* 89, 69–85.
- (52) Sage, D. P., Kulczar, C., Roth, W., Liu, W., and Knipp, G. T. (2014) Persistent pharmacokinetic challenges to pediatric drug development. *Front. Genet.* 5, 281.

(53) O'Hara, K., Wright, I. M., Schneider, J. J., Jones, A. L., and Martin, J. H. (2015) Pharmacokinetics in neonatal prescribing: evidence base, paradigms and the future. *Br. J. Clin. Pharmacol.* 80 (6), 1281–8.

(54) Chadwick, E. G., Capparelli, E. V., Yogev, R., Pinto, J. A., Robbins, B., Rodman, J. H., Chen, J., Palumbo, P., Serchuck, L., Smith, E., and Hughes, M. (2008) Pharmacokinetics, safety and efficacy of lopinavir/ritonavir in infants less than 6 months of age: 24 week results. *AIDS* 22 (2), 249–55.

(55) Urien, S., Firtion, G., Anderson, S. T., Hirt, D., Solas, C., Peytavin, G., Faye, A., Thuret, I., Leprevost, M., Giraud, C., Lyall, H., Khoo, S., Blanche, S., and Tréluyer, J. M. (2011) Lopinavir/ritonavir population pharmacokinetics in neonates and infants. *Br. J. Clin. Pharmacol.* 71 (6), 956–60.

(56) Nikanjam, M., Chadwick, E. G., Robbins, B., Alvero, C., Palumbo, P., Yogev, R., Pinto, J., Hazra, R., Hughes, M. L., Heckman, B. E., and Capparelli, E. V. (2012) Assessment of lopinavir pharmacokinetics with respect to developmental changes in infants and the impact on weight band-based dosing. *Clin. Pharmacol. Ther.* 91 (2), 243–9.

(57) Beath, S. V. (2003) Hepatic function and physiology in the newborn. *Seminars in Neonatology* 8 (5), 337–346.

(58) Grijalva, J., and Vakili, K. (2013) Neonatal liver physiology. *Semin Pediatr Surg* 22 (4), 185–9.